Med. J. Cairo Univ., Vol. 90, No. 4, June: 1179-1186, 2022
www.medicaljournalofcairouniversity.net

Role of Diffusion Kurtosis Imaging in Grading of Brain Gliomas

AHMED ABDEL KHALEK, M.D.*; GEHAD ABDALLA, M.Sc.*; TAREK YOUSRY, M.D.** and MAGDY SETTEIN, M.D.*

The Department of Radiology, Mansoura University Hospitals, Mansoura, Egypt and Neuroradiology Department**, National Hospital for Neurology and Neurosurgery UCL Hospitals NHS Trust, London, UK*

Abstract

Background: Since the 2016 WHO classification, the mutation status of the encoding gene of Isocitrate-dehydrogenase enzyme (IDH) is an important element in the integrated diagnosis of gliomas. Diffusion Kurtosis imaging (DKI) has been used to assess the microstructure of brain tissue as well as gliomas by quantifying the water molecules' non-Gaussian distribution.

Aim of Study: This study aimed in this study to try to elucidate the diagnostic performance of DKI in the characterisation of brain gliomas and its role in the identification of IDH mutation status among different glioma subtypes.

Patients and Methods: 48 patients with histopathological-proven gliomas were included in this prospective study. Diffusion images were obtained on a 3T system with 10/ 30/ 60 diffusion gradient directions with b-value of 300-2500 sec/mm^2. Kurtosis analysis was performed using the Diffusional Kurtosis Estimator software, and segmentation was manually drawn on the co-registered FLAIR-DTI images. The mean value of the "mean kurtosis (MK)" and "mean diffusivity (MD)" were extracted from the solid tumour component and from the contralateral normal-appearing white matter. We then correlated MK and MD with the 2016 CNS WHO tumor grades using statistical software STATA, V15.

Results: Most of the DKI parameters were able to stratify CNS gliomas both according to the 2007 and 2016 WHO classification. MK and MD significantly differed between IDH-mutant and IDH-wt gliomas. In those patients with a lack of 1p/19q codeletion all MKn, MK, MDn, MD significantly differed (p<0.007).

Conclusion: DKI enables the differentiation of gliomas according to the WHO 2016 integrated diagnosis. This would be confirmed after soaring up and standardization of the technique in further research studies.

Key Words: *Diffusion kurtosis – Grading of brain gliomas.*

Introduction

DWI is helpful in glioma imaging by quantifying water molecules' mobility on the assumption of unrestricted but possibly hindered-random diffusion. The likelihood of certain proton diffusing from one location to another in a given time (known as the probability distribution function [PDF]) herein is thought to be Gaussian **[1]**. However, it is now known that the diffusion of water molecules within the brain has a paramount difference caused by complex cyto-architecture composed by cell membranes, organelles and discrete compartments, and drifts from the normal Gaussian distribution. Therefore, the real PDF will be more soared up in contrast to the Gaussian PDF. The widely approved diffusion metrics in tumours, namely the apparent diffusion coefficient (ADC), is limited to detect this deviation from normal Gaussian distribution. A novel diffusion model known as diffusional kurtosis imaging (DKI) is a dimensionless metric and it has recently evolved to quantify the degree of non-Gaussian diffusion of water molecules **[1]**, [2]. Thus, DKI can provide a more realistic data that illustrate brain micro-environment's complexity [3].

DKI is simply considered a continuation of the diffusion tensor imaging (DTI) model, and at least two non-zero diffusion gradient factors (b values) in more than 15 nonlinear diffusion directions are required to acquire both the kurtosis metrics [(radial kurtosis (Kr), axial kurtosis (Ka) and mean kurtosis (Mk)] and diffusion tensor metrics [(mean diffusivity (MD) and fractional anisotropy (FA)] simultaneously **[2]**. Ka is parallel to the first diffusion eigenvector and is believed to be evidence of axonal integrity, while Kr is perpendicular to the first eigenvector plane and is thought to detect myelin integrity. The Mk represents the average diffusional kurtosis coefficient in all diffusion directions and it is assumed to be the principle kurtosis metric which can mirror brain micro-structure **[1,2,4]**.

Correspondence to: Dr. Ahmed Abdel Khalek, The Department of Radiology, Mansoura University Hospitals, Mansoura, Egypt

Through estimating the deviation from Gaussian diffusion, DKI is assumed to translate a biological tissue microenvironment and histological details. Therefore, it is believed that differences in DKI values are resulting from restricted diffusion by cell organelles and membranes, in addition to varying water compartments between intra and extracellular spaces. As brain gliomas' microenvironment is altered according to each particular grade and degree of aggressiveness, DKI is thought to have obvious diagnostic implications in staging and differentiation of gliomas [1,5].

Current evidence shows that robust and precise characterisation of gliomas has become crucial for successful management strategies and outcome predilection. In the light of WHO classifications of brain gliomas, the old 2007 classification depended mainly on the histopathologic features of the tumour and essentially stratifying brain gliomas into more aggressive high-grade and less aggressive low-grade gliomas [6]. While the recent recognition of key genetic markers that also influences the tumour's behaviour rather than only its cellular lineage, has deemed the development of the revised 4th edition of the WHO 2016 classification. One of these key genetic markers is the Isocitrate dehydrogenase (IDH) gene which plays a pivotal role in tumour's angiogenesis, cellularity and metabolism [7]. Therefore, IDH mutation status has gained a particular recognition in the revised 2016 classification and has essentially contributed to the stratification of brain gliomas in to IDH mutant gliomas which show better prognosis and IDH wild type ones with worse outcomes [8].

Inspite of the advent of this revised classification, it still relies on the invasive neurosurgical tissue sampling as a gold standard, that exposes the patient to the burden of post procedural complications, in addition to sampling errors and inconsistency due to intra-tumoural heterogeneity [5]. These limitations indicate a desperate need for a non invasive robust biomarker for stratifying brain gliomas. Yet, it is now remarkable that conventional imaging can not solely elucidate tumour's microenviroment in a precise way, particularly in the light of the IDH mutation status of gliomas. Therefore, multiple clinical trials have been investigating the performance of advanced imaging in gliomas' characterisation and particularly the identification of their IDH mutation status [7]. These advanced imaging protocols included mainly MR perfusion, diffusion weighted imaging and MR spectroscopy. However, investigating novel modalities as diffusion kurtosis imaging is still lacking in the literature community. Therefore, we aim in this study to try to elucidate the diagnostic performance of DKI in the characterisation of brain gliomas and its role in the identification of IDH mutation status among different glioma subtypes.

Patients and Methods

Study design:

This prospective and cross-sectional observational study was held as part of a multimodality MRI study that has been approved by the Research Ethics Committee. All patients have provided written informed consent for participating in the multi-parametric imaging study (including diffusional kurtosis imaging) and the subsequent use of the images for the sake of the research.

Participants:

Consecutive non-treated glioma patients presented to the Neuro-oncology multidisciplinary team meeting in the National Hospital for Neurology and Neurosurgery, UK between 2017 and 2019 were recruited to the study. Eligibility criteria included an informed consent from the participant as well. Patients were excluded if they have received any prior treatment, have any contraindication to MRI or MRI contrast agents or being pregnant or breastfeeding.

Imaging acquisition:

Magnetic resonance imaging data were acquired on a 3T Siemens MAGNETOM Prisma MRI system (Erlangen, Germany) with a 64-channel receive-only head coil. Structural images included: (1) pre- and post-gadolinium injection sagittal 3D T1-weighted Sampling Perfection with Application optimized Contrasts using different flip angle Evolution (SPACE) image acquired with field of view (FOV) = 230x230mm^2, acquisition matrix = 256x256, a slab of 192 slices with 0.9mm slice thickness, repetition time (TR)/echo time (TE) = 700/11ms, flip angle mode = T1 var, echo train duration (ETD) = 155ms, turbo factor (TF) = 38, GRAPPA acceleration factor = 2, 3D acceleration factor = 2, bandwidth (BW) = 630 Hz/px and acquisition time (TA) = 4min 23s; (2) a sagittal 3D high-resolution T2-weighted SPACE image acquired acquired with FOV = 282x282mm^2, acquisition matrix = 256x256, a slab of 176 slices with 1.1mm slice thickness, TR/TE = 3200/401ms, flip angle mode = T2 var, ETD = 872ms, TF = 282, GRAPPA acceleration factor = 2, 3D acceleration factor = 2, BW = 751 Hz/px and acquisition time (TA) = 3min 49s; (3) a sagittal 3D high-

resolution fluid attenuated inversion recovery (FLAIR) SPACE image acquired with FOV = 250x250mm^2, acquisition matrix = 256x256, a slab of 176 slices with 1.0mm slice thickness, TR/TE = 5000/502ms, magnetisation preparation = non-selective T2-IR, inversion time (TI) = 1600ms, flip angle mode = T2 var, ETD = 1017ms, TF = 300, GRAPPA acceleration factor = 2, 3D acceleration factor = 1, BW = 751 Hz/px and acquisition time (TA) = 4min 22s.

Diffusion images were axial diffusion-weighted data obtained using a twice-refocused single shot echo-planar imaging sequence, with FOV = 220x 220mm^2, acquisition matrix = 88x88, 54 axial slices with 2.5mm slice thickness and no gap between slices, TR/TE = 3600/79ms, acceleration factor phase encoding = 2, acceleration factor slice = 2, BW = 2030Hz/px, phase encoding (PE) anterior /posterior (A/P), 60 diffusion gradient directions with *b*-value 2500sec/mm^2, 60 diffusion gradient directions with b-value 1800sec/mm^2, 30 diffusion gradient directions with *b*-value 700sec/mm^2, 10 diffusion gradient directions with *b*-value 300sec/ mm^2, 27 acquisitions with *b*-value 0sec/mm^2 and PE=A/P and 4 acquisitions with *b*-value 0sec/mm^2 and PE=P/A.

Imaging processing and post -processing:

Diffusion data were preprocessed using the fsl software package (fsl.fmrib.ox.ac.uk/fsl/fslwiki, FDT toolbox) to correct for image distortions due to susceptibility-induced off-resonance field using the toolboxes topup [Andersson 2003, Smith 2004] and eddy [Jesper 2016].

After preprocessing, 3 Region of interests (ROIs) were performed using the co-registered T2FLAIR images on the entire volume of the solid tumour tissue after excluding cystic or necrotic areas, peritumoural oedema and contralateral normal-appearing white matter (cNAWM). The ROIs were done by a radiologist who was blinded to the histopathologic results. The voxel intensity values of 9 parameters (axial kurtosis Ka, radial kurtosis Kr, mean kurtosis MK, kurtosis fractional anisotropy Kfa, fractional anisotropy FA, axial diffusivity AD, radial diffusivity RD, mean diffusivity MD) were extracted from the overlaid kurtosis maps. kurtosis analysis was performed using the Diffusional Kurtosis Estimator (DKE) software.

Statistical analysis:

Statistical analyses were performed using IBM SPSS Statistics® Version 22 (IBM, Armonk, NY, USA). Normalised values for each parameter; in which Normalised MK = MK within solid tumour/ MK within NAWM were explored in addition to the non normalised data in all comparative studies. Mann Whitney U-test was performed to compare each parameter value between IDH1/2 mutant and IDH-wild type gliomas. Also, to compare between low-grade gliomas (comprising WHO grades I and II) and high-grade gliomas (including grades III and IV) across the extracted kurtosis parameters, Mann whitney U-test was utilised.

Comparisons among IDH-mutant/1p19q retained astrocytoma, IDH-wild/1p19q retained astrocytoma and IDH-mutant/1p19q codeleted oligodendroglioma was done my Kruskal-Wallis test in all kurtosis extracted parameters. If there is identified significant difference (p<0.05), Bonferroni test was performed.

Receiver operator curve was done for the significant results, area under the curve, sensitivity and specificity were derived and cut off values were calculated using the Youden index.

Results

Participants:

68 patients with suspected glioma were initially recruited to the study. Advanced multiparametric MRI examination was performed after patient's informed consent. Out of the included cohort 20 were male, while female patients were 28. Mean age (standard deviation) of participants with IDH-mutant gliomas and IDH-wild ones was 40.1(11.4) and 49.8(19.8) with no significant difference between the two groups (p=≥0.051). While age differs significantly between low and high-grade glioma' patients [mean age (SD)=38.1(11.8) and 47.4(14.1), p=0.01]. Mean time interval between the MRI scan and neurosurgical biopsy was 2.7 months (standard deviation=3.3). Flow chart of participants is provided in Fig. (1).

The normalised mean values of Mean kurtosis (nMK), radial kurtosis (nKrad) and axial kurtosis (nKax) were significantly lower in grade II gliomas when compared to grade III (nMK 0.48 ±0.06 vs 0.57±0.16, p=0.005; nKr 0.41 ±0.06 vs 0.48±0.13, p=0.01; nKax 0.58±0.06 vs 0.59±0.21, p=0.004). While the normalised mean values of the fractional anisotropy (nFA) and Mean diffusivity (nMD) have not been able to discriminate among any of the glioma grades. Moreover, differentiation between grade II and grade IV was not capable among all of the kurtosis parameters (Table 1).

As regards the receiver operator curve (ROC) analysis, the cut off values for nMK, nKrad and nKax in differentiating grade II from grade III gliomas were: 0.58, 0.57 and 0.55 respectively with sensitivity/specificity at 75%/67%, 83%/45% and 75%/74% and area under the curve (95% CI) of .720 (0.547-0.894), .728 (0.563-0.894) and .715 (0.537-0.893).

The normalised mean values of MK, Kr, FA and MD differed significantly between the IDH wild type and IDH mutant gliomas - both with retained 1p19q - (p: 0.02, 0.009, <0.001 and <0.001 respectively). Meanwhile, non-normalised MK and Kax were not capable of predicting the IDH mutation status within the tumours (p=0.07 and 0.12 respectively). Table (2).

All parameters displayed moderately high diagnostic accuracy, particularly nMD and nMK; which were 91% and 82% respectively. Cut off values for differentiating IDH wild from IDH mutant gliomas, sensitivity, specificity and AUC are available in Table (3).

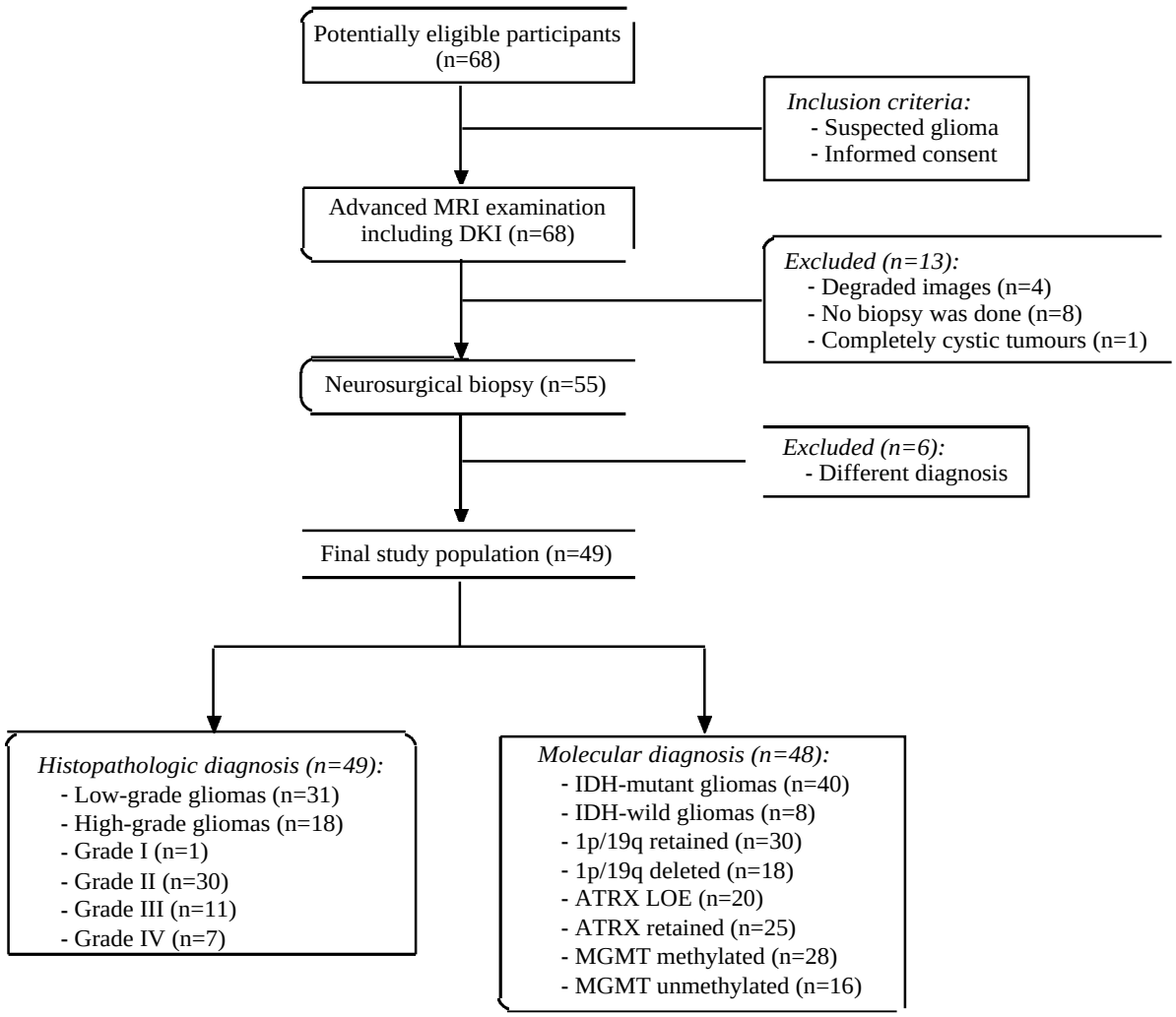

Fig. (1): Flow chart of participants.

Table (1): Normalized metrics association with gliomas' histopathologic grades.

Normalized mean	Grade			Test of significance (Overall)	Post Hoc Tukey test
	2	3	4		
K mean Mean ± SD	0.485±0.061	0.578±0.162	0.505±0.06	F=4.436 p=0.017*	p_1=0.005* p_2=0.561 p_3=0.079
K rad Mean ± SD	0.415±0.062	0.489±0.137	0.426±0.055	F=3.432 p=0.04*	p_1=0.012* p_2=0.701 p_3=0.100
K ax Mean ± SD	0.580±0.06	0.598±0.211	0.618±0.073	F=4.606 p=0.015*	p_1=0.004* p_2=0.387 p_3=0.118
Fa Mean ± SD	0.349±0.081	0.324±0.129	0.323±0.095	F=0.431 p=0.652	p_1=0.451 p_2=0.483 p_3=0.983
D mean Mean ± SD	1.92±0.34	1.78±0.44	1.88±0.491	F=0.543 p=0.584	p_1=0.302 p_2=0.800 p_3=0.561

F: One Way ANOVA test.
*Statistically significant.
p1: Difference between grade 2 & 3.
p2: Difference between grade 2 & 4.
p3: Difference between grade 3 & 4.

Table (2): Normalized metrics association with molecular type of gliomas.

Normalized mean	Type			Test of significance (Overall)	Post Hoc Tukey test
	Wild pqret	Mut pqret	Mut pqdel		
K mean Mean ± SD	0.551±0.055	0.464±0.06	0.557±0.129	F=6.66 p=0.003*	p_1=0.02* p_2=0.861 p_3=0.001*
K rad Mean ± SD	0.477±0.063	0.390±0.06	0.478±0.103	F=8.06 p=0.001*	p_1=0.009* p_2=0.971 p_3=0.001*
K ax Mean ± SD	0.649±0.056	0.565±0.064	0.669±0.174	F=4.84 p=0.012*	p_1=0.074 p_2=0.691 p_3=0.005*
Fa Mean ± SD	0.427±0.09	0.295±0.08	0.365±0.091	F=8.88 p=0.001*	p_1<0.001* p_2=0.084 p_3=0.009*
D mean Mean ± SD	1.53±0.11	2.12±0.36	1.68±0.26	F=17.23 p<0.001*	p_1<0.001* p_2=0.248 p_3<0.001*

F: One Way ANOVA test.
*Statistically significant.
p1: Difference between wild pqret & mut pqret.
p2: Difference between wild pqret & mut pqdel.
p3: Difference between mut pqret & mut pqdel.

Table (3): Diagnostic performance of normalised DKI parameters in differentiating IDH wild type from IDH mutant gliomas.

	AUC (95%CI)	p-value	Cut off point	Sensitivity %	Specificity %	Accuracy %
Normalized.kmean	0.885 (0.774-0.996)	0.001*	0.5014	87.5	80.8	82.4
Normalized.krad	0.865 (0.744-0.987)	0.002*	0.4186	87.5	80.8	82.4
Normalized.kax	0.856 (0.730-0.980)	0.003*	0.5923	87.5	76.9	79.4
Normalized.fa	0.894 (0.786-1.0)	.001*	0.3302	87.5	73.1	76.5
Normalized D mean	0.933 (0.845-1.0)	<0.001*	1.6479	87.5	92.3	91.2

Fig. (2): 29 year old female patient, with IDH mutant, 1p19q retained glioma, loss of expression of ATRX and low MGMT methylation. Histopathology revealed grade II glioma.

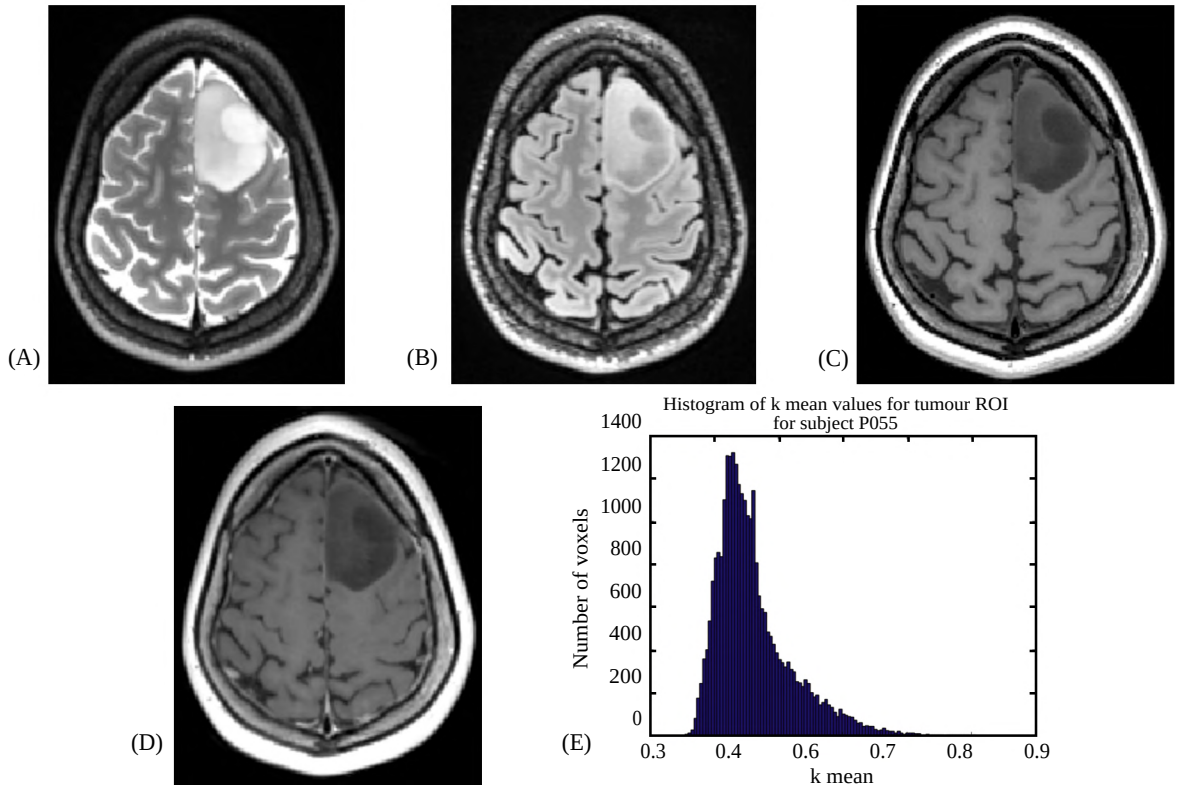

(A) T2w, (B) T2FLAIR, (C)T1w without contrast, (D) T1w with contrast, (E) Histogram values of MK through the tumour. T2/FLAIR mismatch sign is shown in A&B images within the left frontal lobe mass. Tumour is non-enhancing. Mean kurtosis values histogram shows homogenous distribution around low values denoting less complexity of the tumour.

Fig. (3): 31 year old female patient, with IDH mutant, 1p19q retained glioma, loss of expression of ATRX and MGMT unmethylation. Histopathology revealed grade II glioma.

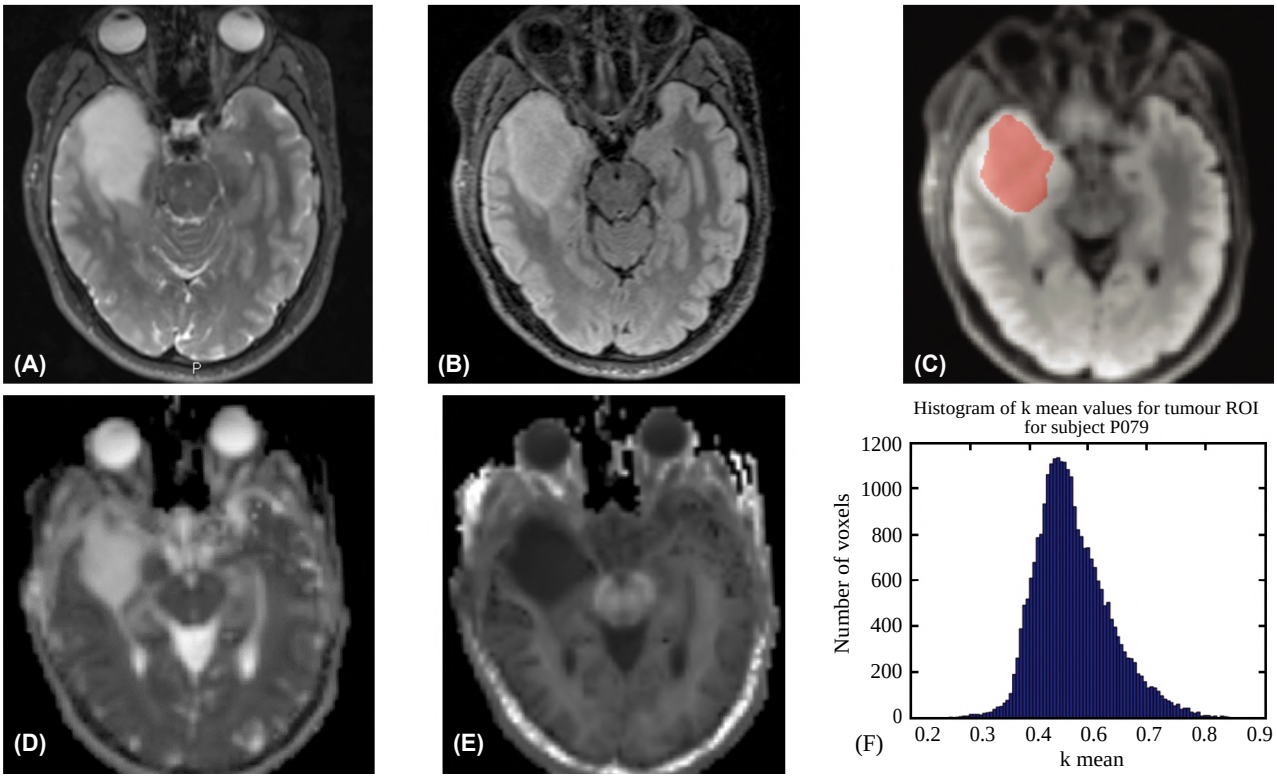

(A) T2w, (B) T2FLAIR, (C) ROI in solid tumour volume in co-registered FLAIR, (D) Mean diffusivity map, (E) Mean kurtosis map (F) Histogram values of MK through the tumour. T2/FLAIR mismatch sign is shown in A&B images. Tumour involving the right temporal lobe is homogenously high in MD and lowin MK. Mean kurtosis values histogram shows homogenous distribution around low values denoting less complexity of the tumour.

Discussion

In our study, we have investigated the role of DKI in stratifying brain gliomas, both according to the histopathologic 2007 grading scheme and the 2016 integrated molecular diagnosis. Our results have shown that the normalised DKI parameters (MK, Krad and Kax) can significantly differentiate between grade II and grade III gliomas rather than other DTI metrics (MD or FA); which have not reached the statistical significant values in discriminating among any of the glioma's grades. Our results are in agreement with previous studies (Raab et al., 2010; Van Cauter et al., 2012); where they have demonstrated that kurtosis derived metrics were superior to the other DTI values in the differentiation of grade II versus III gliomas in the former and high grade versus low grade tumours in the latter.

Albeit, we were not capable of differentiating between grade II and IV or grade III and IV gliomas via any of the DKI parameters. These findings disagree with Raab et al. and Van Cauter et al., work. This could be explained by variations in image acquisition, processing software and the participants' characteristics in the different research methodology.

Moreover, considering the 2016 molecular integrated diagnosis, we have demonstrated that the normalised values of MK, Krad, FA and MD can significantly identify the IDH mutation status within CNS gliomas with diagnostic accuracy of 82.4%, 82%, 76.5% and 91% respectively. Our results agree with previous studies, which illustrated the statistical significance of DKI derived parameters in identifying the IDH mutation status in gliomas. (J-M Hempel, Schittenhelm, et al., 2017; J. Hempel et al., 2016; Zhao et al., 2019). Yet, they have concluded that MK displayed better accuracy than MD on the contrary to our results. Our explanation for this is the smaller number of our cohort, particularly the IDH-wild type group, yet this might represent the normal prevalence of this molecular subtype in the population.

Conclusion:

Diffusion kurtosis imaging is a novel MRI technique that demonstrated very promising performance in the diagnosis of CNS gliomas, particularly in lights of the integrated molecular diagnosis. However, it still lacks standardisation, allowing for the fluctuant acquisition and processing techniques available currently in the literature. Therefore, we assume that further original research work on larger study cohort might fasten the process of its standardisation and hence integration into the imaging protocols of CNS gliomas.

References

1- VAN CAUTER S., VERAART J., SIJBERS J., PEETERS R.R., HIMMELREICH U., DE KEYZER F., et al.: "Gliomas: Diffusion kurtosis MR imaging in grading," Radiology, Vol. 263, No. 2, pp. 492-501, May 2012, doi: http://dx.doi.org/10.1148/radiol.12110927.

2- JIANG R., JIANG J., ZHAO L., ZHANG J.J., ZHANG S., YAO Y., et al.: "Diffusion kurtosis imaging can efficiently assess the glioma grade and cellular proliferation," Oncotarget, Vol. 6, No. 39, pp. 42380-42393, Dec. 2015, doi: http://dx.doi.org/10.18632/oncotarget.5675.

3- HEMPEL J.-M., SCHITTENHELM J., BRENDLE C., BENDER B., BIER G., SKARDELLY M., et al.: "Histogram analysis of diffusion kurtosis imaging estimates for in vivo assessment of 2016 WHO glioma grades: A cross-sectional observational study," European Journal of Radiology, Vol. 95, pp. 202-211, Oct. 2017, doi: http://dx.doi.org/10.1016/j.ejrad.2017.08.008.

4- RAAB P., HATTINGEN E., FRANZ K., ZANELLA F. E., LANFERMANN H., P. R., et al.: "Cerebral gliomas: Diffusional kurtosis imaging analysis of microstructural differences," Radiology, Vol. 254, No. 3, pp. 876-881, Mar. 2010, doi: http://dx.doi.org/10.1148/radiol.09090819.

5- HEMPEL J.-M., BISDAS S., SCHITTENHELM J., BRENDLE C., BENDER B., WASSMANN H., et al.: "In vivo molecular profiling of human glioma using diffusion kurtosis imaging.," Journal of neuro-oncology, Vol. 131, No. 1, pp. 93-101, Jan. 2017, doi: 10.1007/s11060-016-2272-0.

6- LOUIS D.N., OHGAKI H., WIESTLER O.D., CAVENEE W.K., BURGER P.C., JOUVET A., et al.: "The 2007 WHO Classification of Tumours of the Central Nervous System," Acta Neuropathologica, Vol. 114, No. 2, pp. 97-109, 2007, doi: 10.1007/s00401-007-0243-4.

7- HYUN SUH C., SUNG KIM H., CHAI JUNG S., GON CHOI C., and JOON KIM S.: "Imaging prediction of isocitrate dehydrogenase (IDH) mutation in patients with glioma: A systemic review and meta-analysis," doi: 10.1007/s003 30-018-5608-7.

8- LOUIS D.N., PERRY A., REIFENBERGER G., VON DEIMLING A., FIGARELLA-BRANGER D., CAVENEE W.K., et al.: "The 2016 World Health Organization Classification of Tumors of the Central Nervous System: A summary". Acta neuropathologica, Vol. 131, No. 6, pp. 803-20, Jun. 2016, doi: 10.1007/s00401-016-1545-1.

دور التصوير الكورتوسى المنتشر فى تصنيف الأورام الدبقية الدماغية

الخلفية : منذ تصنيف منظمة الصحة العالمية لعام ٢٠١٦، تعد حالة الطفرة فى جين ترميز إنزيم إيزوسترات – ديهيدروجينيز (IDH) عنصراً مهماً فى التشخيص المتكامل للأورام الدبقية. تم استخدام تصوير التفرطح المنتشر (DKI) لتقييم البنية الدقيقة لأنسجة المخ وكذلك الأورام الدبقية عن طريق تحديد التوزيع غير الغاوسى لجزيئات الماء. لذلك نفترض أن DKI يمكنه تحديد حالة IDH للأورام الدبقية.

المنهجية : تم تضمين ٤٨ مريضاً يعانون من أورام دبقية مثبتة نسيجياً فى هذه الدراسة. تم الحصول على صور الانتشار على نظام 3T مع اتجاهات تدرج انتشار ١٠/٣٠/٦٠ بقيمة ٢٥٠٠–٣٠٠ b ثانية مم٢. تم إجراء تحليل التفرطح باستخدام برنامج Kurtosis Estimator Diffusional، وتم رسم التجزئة يدوياً على التسجيل المشترك صور FLAIR-DTI. تم استخراج القيمة المتوسطة لـ التفرطح المتوسط (MK) ومتوسط الإنتشار (MD) من مكون الورم الصلب ومن المادة البيضاء التى تظهر بشكل طبيعى المقابل. ثم قمنا بربط MK و MD بدرجات ورم CNS WHO لعام ٢٠١٦ باستخدام البرنا مج الإحصائى STATA ,V15.

النتائج : تمكنت معظم معلمات DKI من تصنيف الأورام الدبقية فى الجهاز العصبى المركزى وفقاً لتصنيف منظمة الصحة العالمية لعامى ٢٠٠٧ و ٢٠١٦. اختلف MK و MD بشكل كبير بين الأورام الدبقية IDH-mutant و IDH-wt. فى هؤلاء المرضى الذين يعانون من نقص فى حذف كود 1p/19q، اختلفت جميع MKn و MK و MDn و MD اختلافاً كبيراً ($p<0.007$).

الخلاصة : DKI يمكن من تمييز الأورام الدبقية وفقاً للتشخيص المتكامل لمنظمة الصحة العالمية ٢٠١٦. سيتم تأ كيد ذلك بعد رفع مستوى التقنية وتوحيدها فى مزيد من الدراسات البحثية.